Multi-year La Niña events and multi-season drought in the Horn of Africa

Weston Anderson[a,b] , Benjamin I. Cook[c,d] , Kim Slinski[a,b] , Kevin Schwarzwald[e] , Amy McNally[b,f] , and Chris Funk[g] ,

[a] *Earth System Science Interdisciplinary Center, University of Maryland, College Park, MD*
[b] *NASA Goddard Space Flight Center, Greenbelt, MD*
[c] *NASA Goddard Institute for Space Studies, New York, NY*
[d] *Lamont-Doherty Earth Observatory, Palisades, NY* [e] *International Research Institute for Climate and Society, Palisades, NY* [f] *United States Agency for International Development, Washington, DC* [g] *Climate Hazards Center, University of California, Santa Barbara, Santa Barbara, CA*

Corresponding author: Weston Anderson, weston.anderson@nasa.gov

Early Online Release: This preliminary version has been accepted for publication in *Journal of Hydrometeorology*, may be fully cited, and has been assigned DOI 10.1175/JHM-D-22-0043.1. The final typeset copyedited article will replace the EOR at the above DOI when it is published.

ABSTRACT: One of the primary sources of predictability for seasonal hydroclimate forecasts are sea surface temperatures (SSTs) in the tropical Pacific, including the El Niño Southern Oscillation. Multi-year La Niña events in particular may be both predictable at long lead times and favor drought in the bimodal rainfall regions of East Africa. However, SST patterns in the tropical Pacific and adjacent ocean basins often differ substantially between first- and second-year La Niñas, which can change how these events affect regional climate. Here, we demonstrate that multi-year La Niña events favor drought in the Horn of Africa in three consecutive seasons (OND-MAM-OND). But they do not tend to increase the probability of a fourth season of drought owing to the sea surface temperatures and associated atmospheric teleconnections in the MAM long rains season following second-year La Niña events. First-year La Niñas tend to have both greater subsidence over the Horn of Africa, associated with warmer waters in the West Pacific that enhance the Walker Circulation, and greater cross-continental moisture transport, associated with a warm Tropical Atlantic, as compared to second-year La Niñas. Both the increased subsidence and enhanced cross-continental moisture transport favors drought in the Horn of Africa. Our results provide physical understanding of the sources and limitations of predictability for using multi-year La Niña forecasts to predict drought in the Horn of Africa.

Accepted for publication in *Journal of Hydrometeorology*. DOI 10.1175/JHM-D-22-0043.1.

1. Introduction

Drought has been a frequent trigger of acute food insecurity in the Horn of Africa (38E to 53E, 5S to 8N) over the last decade (Anderson et al. 2021; Funk et al. 2018; Maxwell and Hailey 2020; Maxwell and Majid 2016; Shukla et al. 2021). As of February, 2022, portions of the Horn of Africa are experiencing a multi-season drought in which rainfall has been below normal during the short rains (Oct-Dec) of 2020, the long rains (Mar-May) of 2021, and again in the short rains of 2021, which is contributing to the ongoing food security crisis in the region (FEWSNET 2021). In this context, there is considerable interest in the potential to understand and predict such multi-year drought events at lead times beyond the seasonal timescale, which would allow governments and humanitarian aid agencies to better prepare for the acute food insecurity caused by consecutive seasonal droughts.

One of the primary sources of predictability for seasonal hydroclimate forecasts are sea surface temperatures (SSTs) in the tropical Pacific, including the El Niño Southern Oscillation (ENSO) (Lenssen et al. 2020; Shukla et al. 2019; Funk et al. 2018). Operational seasonal forecasting systems, such as the North American Multi-Model Ensemble (NMME), demonstrate skill in predicting Niño3.4 anomalies at leads up to 8-12 months in advance (Barnston et al. 2019, 2012). And while NMME forecasts are not available for leads longer than 12 months, machine learning-based multi-year forecasts of Niño3.4 anomalies demonstrate skill up to 16 months in advance (Ham et al. 2019). Such forecasts of tropical Pacific SSTs are relevant for forecasting drought in East Africa during both the Oct-Dec and Mar-May season. Indeed, operational NMME precipitation forecasts are more skillful during strong ENSO years in East Africa (Shukla et al. 2019).

La Niña events in particular may be predictable multiple years in advance provided the correct initial conditions (Wu et al. 2021; DiNezio et al. 2017a,b; Luo et al. 2017). It has long been recognized that both El Nño and La Niña exhibit a life cycles with predictable periods of growth and decay that are phase locked to the seasonal cycle (Zebiak and Cane 1987; Rasmusson and Carpenter 1982). Recently, it has been identified that La Niñas are more likely to persist for two years as compared to El Niños (Okumura and Deser 2010). This multi-year persistence of La Niña is particularly pronounced immediately following strong El Niños, when subsurface oceanic heat content is discharged off the equator, the thermocline in the tropical Pacific is strongly shoaled in the east Pacific, and the warming of the Atlantic and Indian Oceans acts to enhance the easterly winds in the central Pacific (DiNezio and Deser 2014; Wu et al. 2019). The cycle of strong El Niños being followed by multi-year La Niñas represents a signal that may be predictable up to two years in advance (Wu et al. 2021; DiNezio et al. 2017a,b; Luo et al. 2017), although to date operational forecasts are not regularly issued at these lead times.

Accepted for publication in *Journal of Hydrometeorology*. DOI 10.1175/JHM-D-22-0043.1.

Multi-year La Niñas are not only potentially predictable, but they are also detrimental to agriculture in the bimodal rainfall regions of East Africa, where La Niñas strongly favor drought during the short rainy season (Oct-Dec) and may also favor drought during the long rainy season (Mar-May). The negative phase of the Indian Ocean Dipole and La Niña, which often occur together, favor drought during the short rains by strengthening the Indian Ocean branch of the Walker Circulation (Liebmann et al. 2014; Liu et al. 2020; Blau and Ha 2020; Goddard and Graham 1999; Tierney et al. 2013; Dutra et al. 2013). Rainfall is suppressed under these conditions because convection and atmospheric ascent over the West Pacific is enhanced while over the Western Indian Ocean and the Horn of Africa atmospheric descent intensifies and suppresses convection. During the Mar-May long rains, the connection between rainfall in the Horn of Africa and SSTs is more complex. Historically, ENSO has had no significant teleconnection to the long rains (Nicholson 2017), although recent research has demonstrated that a warm West Pacific and cold east/central Pacific can force drought in the Horn of Africa by strengthening the Walker Circulation (Funk et al. 2019, 2018; Ummenhofer et al. 2018; Williams and Funk 2011; Hoell and Funk 2013, 2014; Liebmann et al. 2017; Lyon and DeWitt 2012; Funk and Hoell 2015) and modifying moisture fluxes into the region (Hoell and Funk 2013). The combination of La Niñas with warm West Pacific sea surface temperatures and the negative phase of the Indian Ocean Dipole, therefore, has the potential to force consecutive years of drought (Hoell and Funk 2014) similar to the present multi-year drought in the region. In 2015/16, for example, a strong El Niño followed by consecutive La Niñas led to substantial food insecurity in Eastern and Southern Africa Funk et al. (2018)

However, SST patterns in the tropical Pacific and adjacent ocean basins often differ substantially between first- and second-year La Niñas, which can change how these events affect regional climate. First-year La Niñas develop following El Niños while second-year La Niñas persist from the previous La Niña. Because of this, SSTs in the central Pacific tend to be colder during first-year events (Wu et al. 2019), while SSTs are warmer and the associated convective heating in the West Pacific is greater during the summer of a developing first-year La Niña as compared to that of a second-year La Niña (Jong et al. 2020). Tropical Atlantic SSTs differ as well, tending to be warmer during first-year La Niñas as compared to second-year La Niñas (Okumura et al. 2017) during Nov-Apr. These differences between first-year and second-year La Niñas have been shown to substantially affect atmospheric teleconnections during boreal winter (Okumura et al. 2017) when ENSO events tend to peak in strength, during boreal summer (Jong et al. 2020) when events are developing, and during boreal spring (Tokinaga et al. 2019) when events are decaying.

Here, we characterize how multi-year and single-year La Niñas affect the probability of consecutive seasons of drought in the Horn of Africa. We will address two main questions in our analysis: (1) How do single- and multi-year La Ninas affect drought occurrence during consecutive rainy

Accepted for publication in *Journal of Hydrometeorology*. DOI 10.1175/JHM-D-22-0043.1.

seasons over east Africa? and (2) How do the mechanisms differ across seasons and single- versus multi-year La Nina events? Improving our understanding of the dynamics of multi-year La Niñas as they relate to drought and water resources in food insecure regions will directly inform the potential usefulness of long-lead ENSO forecasts for these areas. We analyze precipitation due to its importance for rainfed cropping systems and runoff as an integrated metric of moisture supply to pastoral water points and river flow in the region.

2. Methods

For data on precipitation we use both the Global Precipitation Climatology Center (GPCC) version 2020 (Schneider et al. 2018) as well as the Climate Research Unit (CRU) time series v4.05 (Harris et al. 2020), both gridded to 0.5 degrees globally, from 1920-2019. We begin our analysis in 1920 because a greater number of precipitation gauge stations report data after this period, resulting in greater coverage over the Horn of Africa in the gridded GPCC product (SI Figure 1). For data on runoff, we use the GRUN observational-based runoff dataset (Ghiggi et al. 2019), which uses precipitation and temperature reanalyses to train a machine learning model to predict monthly runoff rates. To calculate precipitation and runoff anomalies we first aggregate values to Oct-Dec and Mar-May totals, then calculate differences from the long-term (1949-2019) average, before finally converting to a z-score by dividing by the standard deviation over the same period. Note that using a z-score of three-month seasonal precipitation anomalies is mathematically equivalent to the commonly used three-month standardized precipitation index (SPI). To diagnose circulation anomalies in the post-1950 period, we use the ERA5 global reanalysis (Hersbach et al. 2020) because the precipitation from this reanalysis has been shown to be more accurate in the Horn of Africa as compared to previous reanalyses (Gleixner et al. 2020). We use atmospheric winds and the vertical integral of water vapor flux, which is available as a standard output for ERA5 calculated as the moisture flux in a column of air extending from the surface of the Earth to the top of the atmosphere. We calculate anomalies as differences from the 1950-2020 long term average.

For data on sea surface temperature (SST), we use values from the Hadley Centre Sea Ice and Sea Surface Temperature data set (HadISST) (Rayner et al. 2003). Because there has been significant trends in SST over the 1920-2019 period, we detrend SST values locally by subtracting the low-frequency filtered tropical and subtropical mean SST value. We first calculate the trend by calculating the area-weighted SST value in the 33 S - 33 N region before smoothing the resulting time series with a 30-year low-pass locally weighted scatterplot smoothing (LOWESS) filter, and subtracting this trend from each local SST value. We then remove the average SST value at each point to calculate anomalies before aggregating to seasonal Oct-Dec and Mar-May values.

Accepted for publication in *Journal of Hydrometeorology*. DOI 10.1175/JHM-D-22-0043.1.

We identify La Niña events as years when SST anomalies in the Niño 3.4 region are at least -0.5°C during Oct-Dec. We use the Oct-Dec season to identify events because ENSO events tend to peak during boreal winter and because Oct-Dec is the short rains season, which ensures the identified events had developed by the time of the short rains. We next separate La Niña events into multi-year La Niñas and single-year La Niñas using the same -0.5°C threshold. In this analysis we do not consider the small number of third-year La Niña events on record. While the contemporaneous relationship between Mar-May Niño 3.4 and East African rains is weak (Funk et al. 2018), there have been frequent dry East African long rains following Oct-Dec La Niña events.

From this point forward we will refer to the the first year of a La Niña, regardless of whether it eventually developed into a second-year event, as a 'first-year La Niña' with the associated seasons being 'Oct-Dec of year one' or 'Mar-May of year one' to refer to the short rains coincident with the peak of the event or the long rains during the decaying phase of an event. La Niña events that do not develop into a second-year La Niña will be referred to as 'single La Niñas' while those that do develop into a second consecutive event will be referred to as 'double La Niñas'. The Oct-Dec season coincident with the peak of the second year of a double La Niña will be referred to as 'Oct-Dec of year two' with the following Mar-May being referred to as 'Mar-May of year two'.

To assess statistical significance of La Niña composites of SST, precipitation, and runoff, we use a double bootstrap superposed epoch analysis, as in (Rao et al. 2019). A double bootstrap superposed epoch analysis allows us to evaluate the statistical significance of the La Niña signal while accounting for sample size of our La Niña event set. This approach simultaneously evaluates two questions: (1) How robust is an apparent drought signal within the event set of La Niña years? and (2) how likely are we to observe an equally strong drought signal by drawing the same number of years at random from the full record of all years? The first question addresses the possibility that the observed signal is the result of outliers within the event set of La Niña years, while the second question addresses the possibility that the observed signal would arise by chance alone given the observed number of La Niña years. We first block resample each variable in contiguous three year blocks 1,000 times with replacement from the full 1920-2019 period to create the full 'noise' distribution against which the composite mean will be evaluated. We then resample from each La Niña composite 1,000 times, drawing 75% of events without replacement before calculating the mean of the resampled composite. The subsequent distribution of composite means represent the La Niña event distribution. For each noise and each event distribution we plot the 5th, 10th, 20th, and 80th, 90th, and 95th percentiles.

Accepted for publication in *Journal of Hydrometeorology*. DOI 10.1175/JHM-D-22-0043.1.

3. Results

Twenty-five La Niñas were identified from 1920 to 2019 (Fig. 1a,b). Seventeen of these were first-year La Niñas, of which eight were followed by at least one consecutive year of La Niña. The nine first-year La Niña events that did not develop into a second year of La Niña were 1924, 1933, 1938, 1942, 1945, 1964, 1988, 1995, and 2007. The eight first-year La Niñas that were followed by a second consecutive La Niña were 1949/1950, 1954/1955, 1970/1971, 1973/1974, 1983/1984, 1998/1999, 2010/2011, and 2016/2017. Here the year refers to the Oct-Dec near the peak of each event.

Comparing the Oct-Dec SSTs of the first year of double La Niñas to those of single-year La Niñas (Fig 1a,b) indicates that the former tended to develop from stronger El Niños but tended to be similar in their peak intensity. Double La Niñas were persistently colder during the spring and summer between peak event intensities, often not warming above -0.5°C during the months between La Niña peaks.

We found that both single and double La Niñas affect precipitation and subsequently runoff during the Oct-Dec short rains in the Horn of Africa, consistent with past literature indicating the strong influence of ENSO during the short rains season in the Horn of Africa (Liebmann et al. 2014; Liu et al. 2020; Blau and Ha 2020; Goddard and Graham 1999; Tierney et al. 2013; Dutra et al. 2013) All three kinds of La Niña years - single La Niñas, the first year of double La Niñas, and the second year of double La Niñas - tend to be associated with below normal precipitation and runoff in Oct-Dec (Fig. 1c-f; see also SI Figure 2). The strength of the reduction in precipitation and runoff is greater for the first-year La Niñas as might be expected from the greater intensity of these events as compared to second-year La Niñas, which would more strongly modify the Walker Circulation, resulting in more strongly suppressed convection in the region. The strength of the precipitation response is slightly greater during first-year La Niñas as compared to that of single-year La Niñas, although the reasons for this are unclear.

The Mar-May long rains during the decaying phase of La Niñas demonstrated a greater diversity of precipitation and runoff responses. The Mar-May long rains during the decaying phases of both types of first-year La Niñas were below normal, while the Mar-May long rains following second-year La Niñas tended to be wetter than normal (Fig. 1c,d; SI Figure 2).

Whether these results are robust, however, depends on both the variability of events within each La Niña composite and the variance of the years not included in the composite. We therefore assess the robustness of event composites by using a double-bootstrap superposed epoch analysis (Rao et al. 2019), which subsamples both the La Niña composite itself and the years not included in the La Niña composite to generate confidence estimates around the expected background 'noise' of

Accepted for publication in *Journal of Hydrometeorology*. DOI 10.1175/JHM-D-22-0043.1.

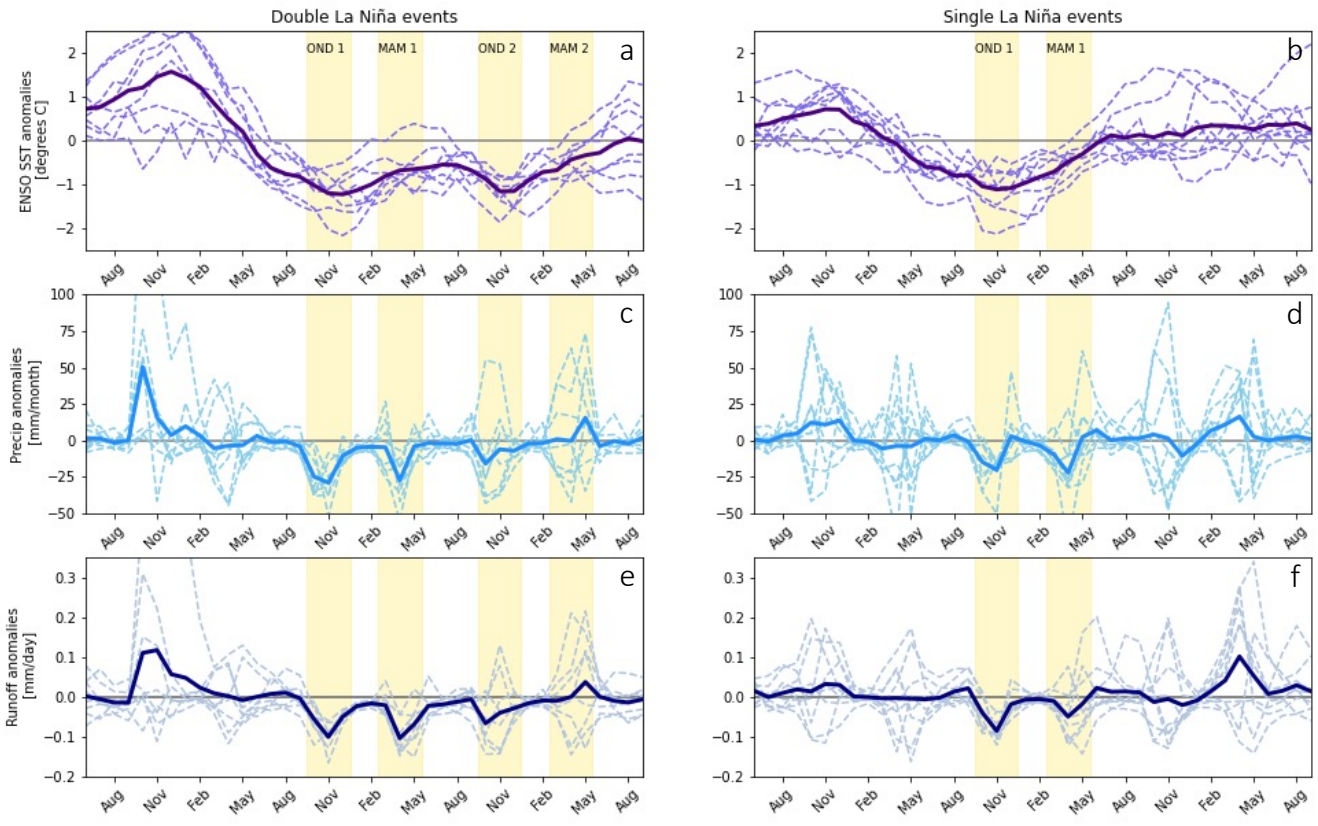

FIG. 1. Sea surface temperature anomalies in the Niño 3.4 region (a,b), precipitation anomalies in the Horn of Africa (c,d), and runoff anomalies in the Horn of Africa (e,f) during first-year and second-year events of multi-year La Niñas (a,c,e) and single-year La Niñas (b,d,f). Individual events shown with dotted lines, composite means shown with solid lines. The Horn of Africa is defined as the region between 38E and 53E and between 5S and 8N.

events not included in the composite as well as a confidence estimate on the La Niña composite mean.

During the short rains season (OND) season, all three types of La Niñas have a distribution of SST composite means that are colder than the 95% confidence interval of the background noise of SSTs (Fig. 2a,b). This is to be expected given that the OND season is the season we use to define the events that are included in the composites. While the first year of a double La Niña tends to be colder than both a second-year and a single-year La Niña, the average composite mean of a first-year event is not outside of the 95% confidence interval of either a second-year or single-year La Niña.

Accepted for publication in *Journal of Hydrometeorology*. DOI 10.1175/JHM-D-22-0043.1.

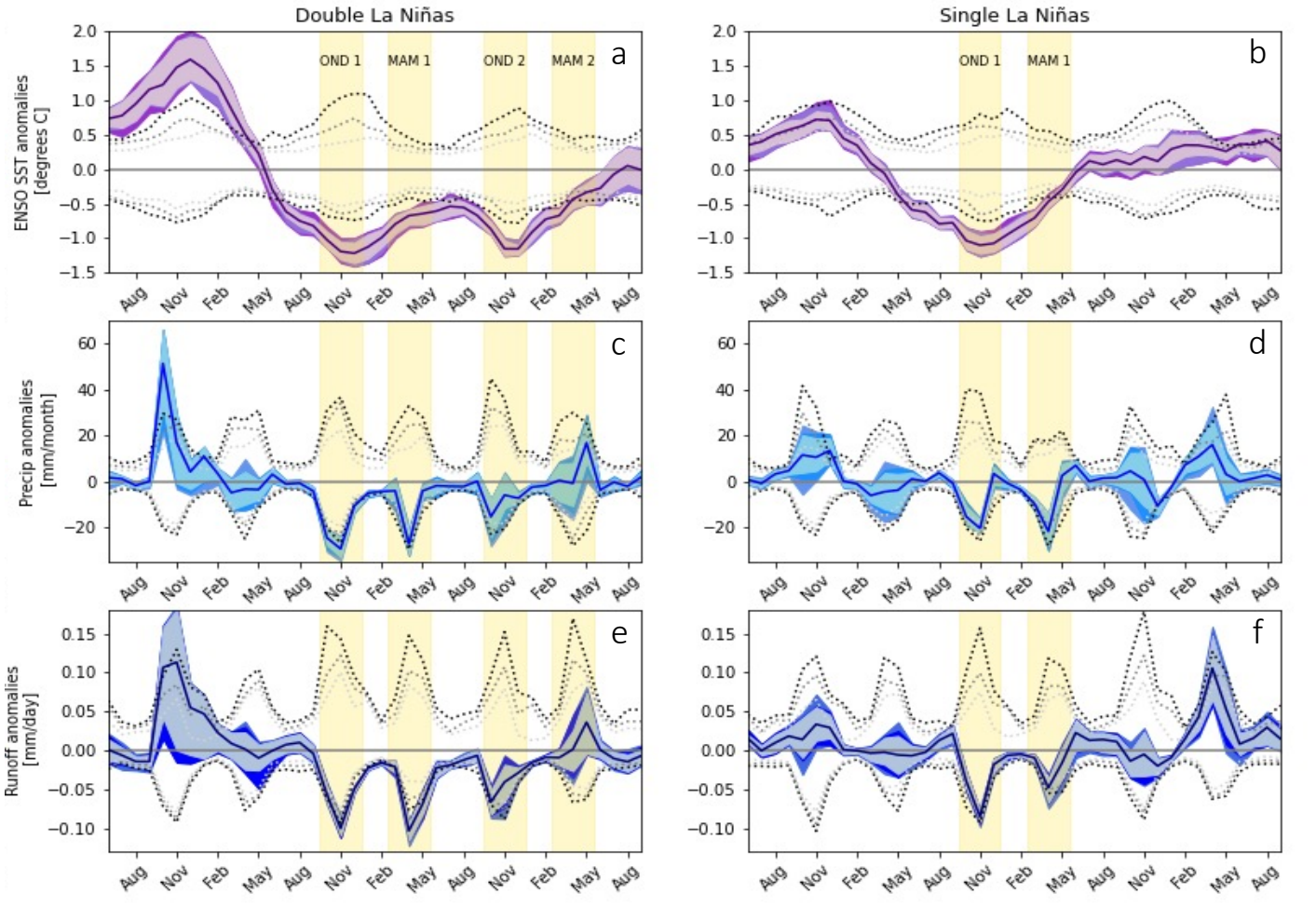

FIG. 2. Uncertainty around composite means from Fig. 1 estimated using a double-bootstrap superposed epoch analysis. Shading shows the 5th, 10th, 20th, and 80th, 90th, and 95th percentiles of the composite mean, while the solid lines are composite means, as in Figure 1 for sea surface temperature anomalies in the Niño 3.4 region (a,b), precipitation anomalies in the Horn of Africa (c,d), and runoff anomalies in the Horn of Africa (e,f) during first-year and second-year events of multi-year La Niñas (a,c,e) and single-year La Niñas (b,d,f). Dotted lines represent bootstrapped uncertainty estimates as the 5th and 95th (black), 10th and 90th (grey), or 20th and 80th (light grey) percentiles of composite means calculated based on years drawn at random from the full record (see methods).

SSTs during the Mar-May season, on the other hand, are more different from one another. SSTs remain significantly lower than the background variability (e.g. the 95% confidence interval of

Accepted for publication in *Journal of Hydrometeorology*. DOI 10.1175/JHM-D-22-0043.1.

the composite mean does not overlap with that of the background variability) after the first year of double La Niñas. This indicates that the tropical Pacific remains significantly colder than normal from March through the end of May between La Niña peaks. SSTs after second-year and single-year La Niña events tend to return to neutral more quickly such that by May the 95% confidence interval of SSTs are within the background 95% confidence interval of the noise distribution in both cases.

Oct-Dec precipitation and runoff are lower than normal during first-year La Niñas of both types, although double La Niña are slightly drier than single-year La Niñas. During first year of a double La Niña, Oct-Dec precipitation and runoff is near the 5th percentile, while during the first year of a single La Niña precipitation and runoff is near the 20th percentile. Oct-Dec rainfall during second-year La Niñas (Figure 2c) also tends to be drier than normal on average, although there is a greater event-to-event difference and they tend to be less dry than first-year events. During second-year La Niñas, the 95% confidence interval of Oct-Dec precipitation and runoff is significantly wider than that of first-year La Niñas. It is generally below zero but not below the 5th percentile of the noise distribution, and the composite mean is not drier than the 20th percentile. These results are similar using CRU TS v4.05 as an alternative gridded precipitation product (SI Fig. 3).

The Mar-May long rains season tends to be dry following first-year events of both types but wet following second-year La Niñas. While the 95% confidence interval of Mar-May precipitation during first-year La Niñas overlaps with the 20th percentile of the noise distribution, that of second-year Mar-May precipitation is centered at or above zero (Figure 2c), depending on the month. This illustrates that not only does Mar-May season following second-year La Niñas tend to be wetter than that following single-year La Niñas, it also tends to be wetter than average.

While Figures 1 and 2 describe the time-evolution of regional-average precipitation over the Horn of Africa, Figures 3 and 4 illustrate the spatial precipitation response. During a first-year La Niña, precipitation deficits are widespread during the Oct-Dec short rains and subsequent Mar-May long rains, although deficits are generally stronger during the first year of a double La Niña. Precipitation deficits during the Oct-Dec short rains of a second-year La Niña are more spatially confined to Southeastern Kenya and Southern Somalia, but are not statistically significant. During the Mar-May long rains following a second-year event, virtually the entire Horn of Africa experiences normal or above-normal rainfall (Fig. 4g,h), although anomalies are again not statistically significant anywhere in the study domain. Individual years for first-year and second-year La Niñas are shown in SI Figs. 4 and 5. Overall, the individual years are heterogeneous, with several extremely wet years (1951, 2018), one exceptionally dry year (2000) and many with mixed anomaly patterns.

The different drought responses during the Oct-Dec short rains during each La Niña type is consistent with observed differences in the Indian Ocean SSTs. During Oct-Dec, the influence of

Accepted for publication in *Journal of Hydrometeorology*. DOI 10.1175/JHM-D-22-0043.1.

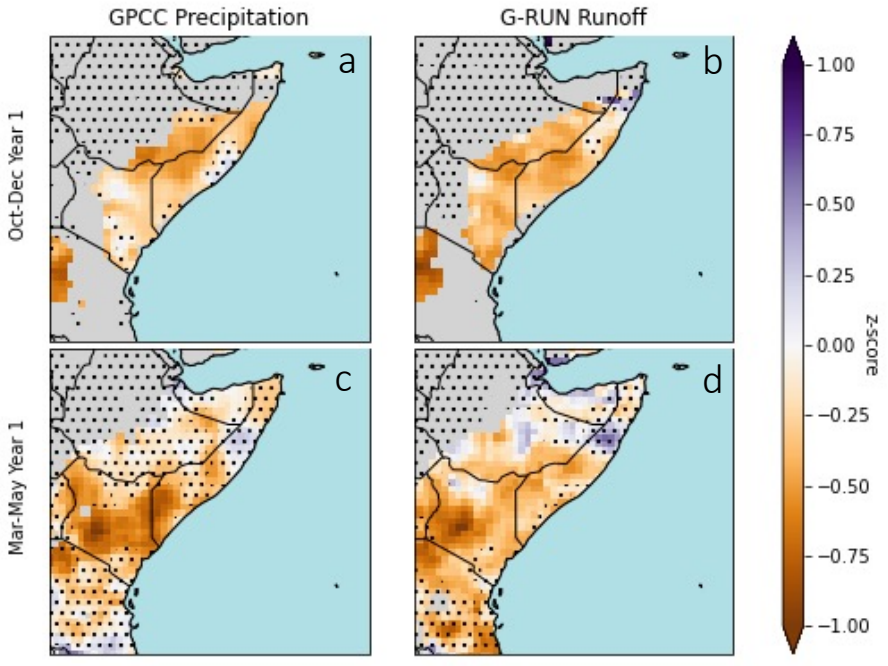

FIG. 3. Average precipitation (a,c) and runoff (b,d) z-scores in the Horn of Africa during single-year La Niñas during the Oct-Dec short rains and the subsequent Mar-May long rains. Grey regions indicate climatologically dry areas, defined as receiving less than 30% of annual precipitation during the plotted months.

the tropical Pacific is mediated by the Indian Ocean (Goddard and Graham 1999). In particular, the negative phase of the Indian Ocean Dipole (IOD) - e.g. warm SSTs in the eastern tropical Indian Ocean and cool SSTs in the western tropical Indian Ocean - acts to reduce precipitation across the Horn of Africa (Saji and Yamagata 2003) due to a suppression of the Indian Ocean branch of the Walker Circulation (Behera et al. 2005). During Oct-Dec of single year La Niñas and the first year of double La Niñas, cold tropical Pacific SSTs co-occur with warm western Pacific SSTs and the negative phase of the IOD (Fig. 5a, c), resulting in widespread and statistically significant reductions in precipitation (Fig. 3a, 4a) and runoff (Fig. 3b, 4b). Both the warm western Pacific SSTs and the negative phase of the IOD act to weaken the Indian Ocean branch of the Walker Circulation. During Oct-Dec of second-year La Niñas, however, neither the warm western Pacific

Accepted for publication in *Journal of Hydrometeorology*. DOI 10.1175/JHM-D-22-0043.1.

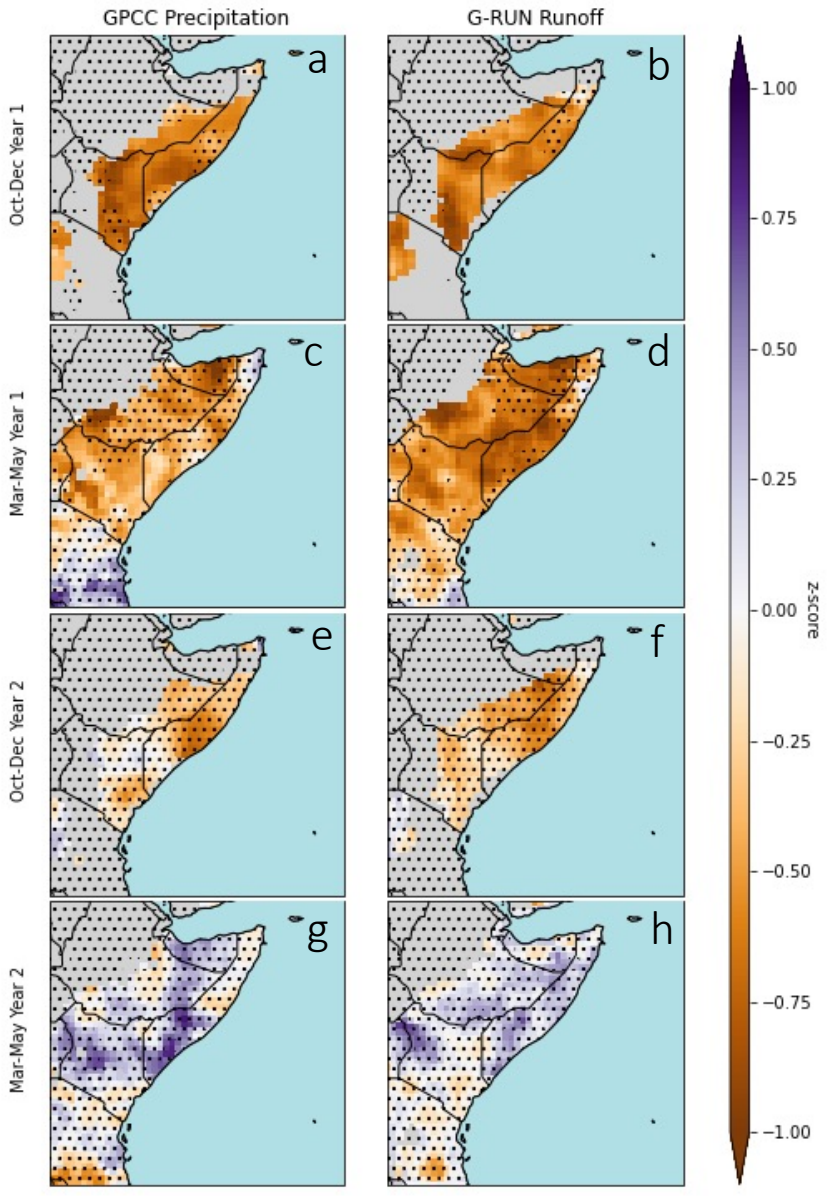

FIG. 4. Average precipitation (a,c,e,g) and runoff (b,d,f,h) z-scores in the Horn of Africa during multi-year La Niñas during the Oct-Dec short rains of first-year events and the subsequent the Mar-May long rains during first-year events (a-d), as well as during the Oct-Dec short rains of second-year events and the subsequent the Mar-May long rains during second-year events (e-h). Grey regions indicate climatologically dry areas, defined as receiving less than 30% of annual precipitation during the plotted months.

SSTs nor the negative IOD are present, resulting in dry but statistically insignificant reductions in precipitation and runoff (Fig. 4e,f) despite the presence of La NiÃśa conditions in the tropical Pacific (Fig. 2a, 5e).

The reasons for the discrepancy between Mar-May rainfall responses following first-year events of both types as compared to second-year La Niñas is not immediately obvious. It is true that the

Accepted for publication in *Journal of Hydrometeorology*. DOI 10.1175/JHM-D-22-0043.1.

Tropical Pacific SST in the Niño 3.4 region during the Mar-May of a first-year event in a double La Niña tends to be cooler than that of a single-year event or than that of a second-year event. But that doesn't explain why the Mar-May rainfall and runoff following a single-year La Niña is drier than that following the second year of a double La Niña, both of which have similar SST values in the Niño 3.4 region (Fig. 2a,b). The double-bootstrap superposed epoch analysis indicates that these differences in rainfall and runoff are unlikely to have occurred by chance. Given this, and provided that there is some indication that all three ocean basins may affect the rainfall in the Horn of Africa long rains, we first investigate the differences in SST anomalies outside of the Niño 3.4 region before linking these SST anomalies to the observed pattern of drought.

Tropical SST anomalies differ considerably during Mar-May following single-year La Niñas, during the first-year of double La Niñas, and during the second year of double La Niñas. During Mar-May after the first-year of double La Niñas (Fig. 5d), the SST in the Tropical Pacific is considerably colder than during either single-year events (Fig. 5b) or second-year events (Fig. 5f). Both single-year events and the first-year of double La Niñas, however, tend to have cold Western Indian Ocean SSTs, warm tropical West Pacific SSTs, and warm tropical Atlantic SSTs. The SST anomalies in the tropical Atlantic and West Pacific during the Mar-May following a second-year event, however, are relatively cooler and not statistically significant. Based on past literature, the differences in Atlantic SST anomalies have the potential to favor drought by enhancing cross-continental moisture transport (Camberlin and Okoola 2003; Okoola 1999a,b), while strong zonal SST gradients in the Pacific and warm West Pacific SSTs are likewise conducive to drought due to an enhanced Walker Circulation (Funk et al. 2019, 2018; Ummenhofer et al. 2018; Williams and Funk 2011; Hoell and Funk 2013, 2014; Liebmann et al. 2017; Lyon and DeWitt 2012). And while the zonal overturning cell associated with the Walker Circulation is less coherent during MAM than OND (Hastenrath et al. 2011), the clear impact of double La Niñas on Mar-May precipitation strength suggests a possible role for the basin-wide vertical circulation. To assess whether these mechanisms support the enhanced probability of drought during first-year as compared to second-year La Niñas, we create composites for winds (Fig. 6) and vertically integrated moisture transport (Fig. 7) using ERA 5 data from 1950-present.

During first-year events of both types, atmospheric ascent is stronger than normal over the warmer than normal Atlantic and West Pacific SSTs, while over the Horn of Africa there is stronger than normal descent in the middle and upper atmosphere (Figure 6a,c). Second-year La Niña events, on the other hand, tended to have enhanced subsidence over the tropical Atlantic rather than enhanced ascent, as well as mid-tropospheric ascent over the Horn of Africa. And while the Mar-May following second-year La Niña events do tend to show slightly enhanced ascent over the West Pacific, it is weaker than during first-year La Niñas and the subsequent anomalous descent tends

Accepted for publication in *Journal of Hydrometeorology*. DOI 10.1175/JHM-D-22-0043.1.

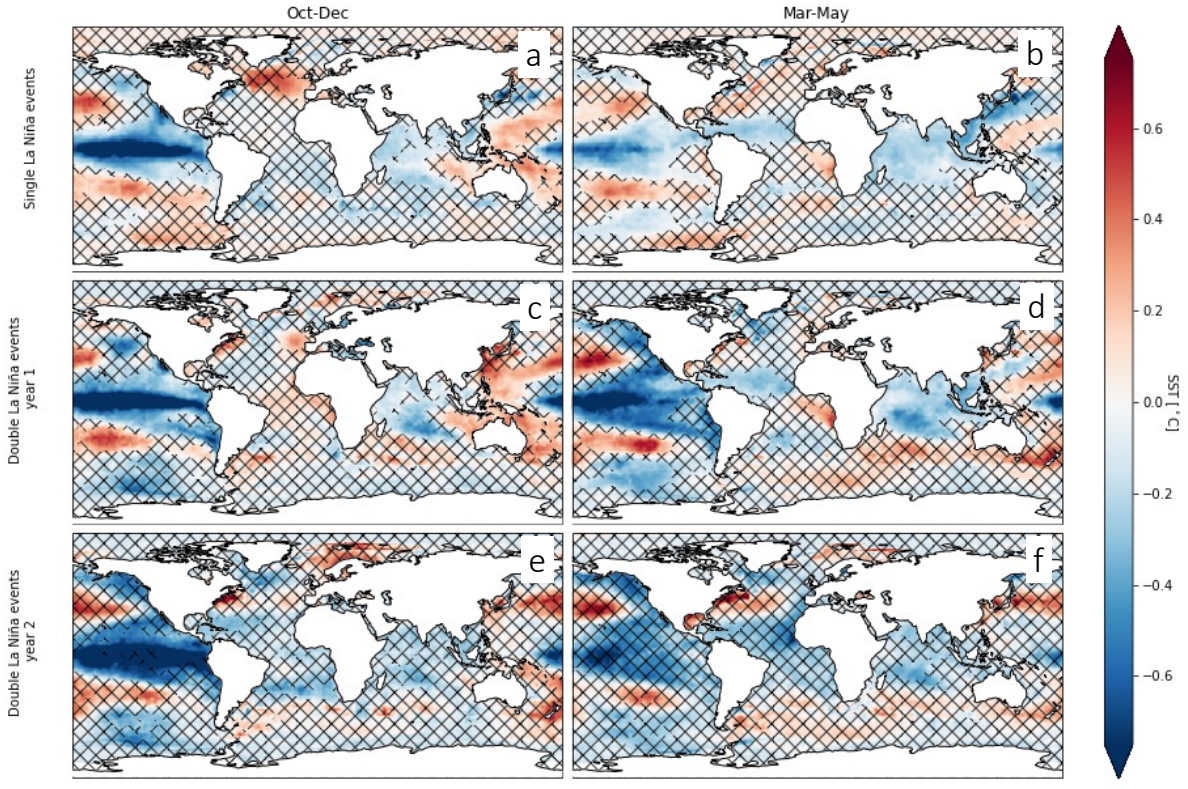

FIG. 5. Sea surface temperature anomalies during the short rains (left column) and long rains (right column) of single-year La Niñas (a,b), as well as during the first-year (c,d) and second-year (e,f) of multi-year La Niñas. Hatching indicates sea surface temperature anomalies that are not significant at the p<0.9 level.

to be over the Eastern tropical Indian Ocean near 80-100E rather than over the Horn of Africa. An eastward-shifted subsidence would be less effective at suppressing convection over the Horn of Africa, consistent with the observed wetter conditions during second-year La Niña events. This result is consistent with that of Hoell et al. (2014) (Hoell et al. 2014), who find that La Niñas that occur with warmer West Pacific SSTs tend to shift the descending branch of the Walker Circulation further west over the Horn of Africa, while those with cooler West Pacific conditions are associated with descent over the Indian Ocean instead. That the long rains following second-year La Niñas tend to be wetter than those following first-year La Niñas, therefore, may be partially the result of a Walker Circulation that is shifted further westward during first-year events as compared to second-year events.

Accepted for publication in *Journal of Hydrometeorology*. DOI 10.1175/JHM-D-22-0043.1.

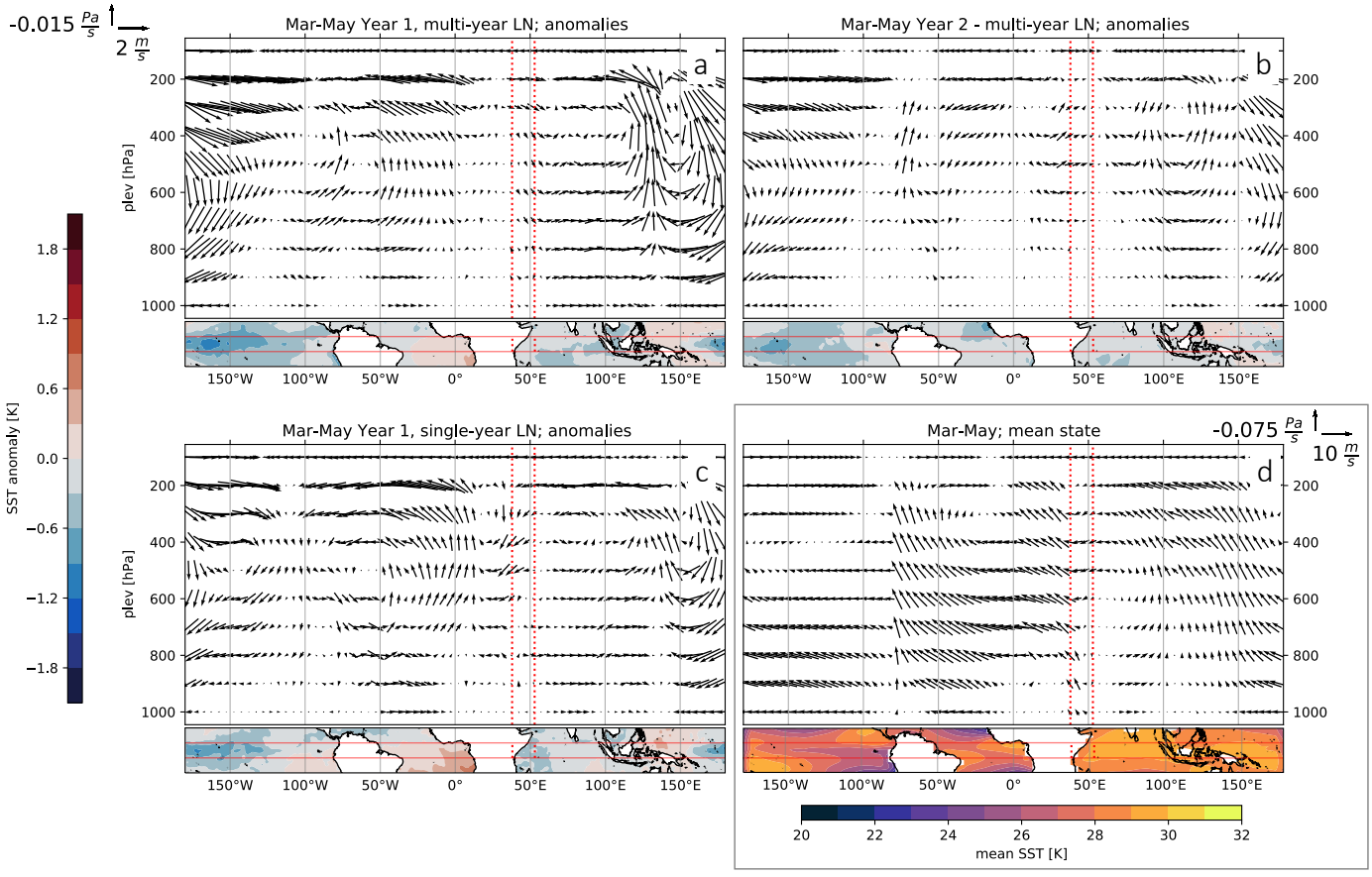

FIG. 6. Atmospheric circulation climatology (top left) and anomalies averaged from 5S to 5N during single-year La Niñas (top right), as well as during the first-year (bottom left) and second-year (bottom right) of multi-year La Niñas.

Figure 7 illustrates the climatological and anomalous vertically integrated moisture transport during the Mar-May long rains following each type of La Niña. Moisture is transported from the southeast into the region before being transported to the west across the continent either over Northern Tanzania or through the Turkana Channel (Fig. 7a,b). During all La Niñas, more moisture than normal is transported into the region from the southeast and more moisture is also diverged out of the region to the northeast. The result of this is that there is little difference between first-year La Niñas and second-year La Niñas in terms of the vertically integrated moisture transport through the North, South, or East boundaries of the region (Fig. 7, calculation not shown). The major difference between the types of La Niñas is in the amount of moisture moved westward across the continent. During first-year events either a normal or greater-than-normal

Accepted for publication in *Journal of Hydrometeorology*. DOI 10.1175/JHM-D-22-0043.1.

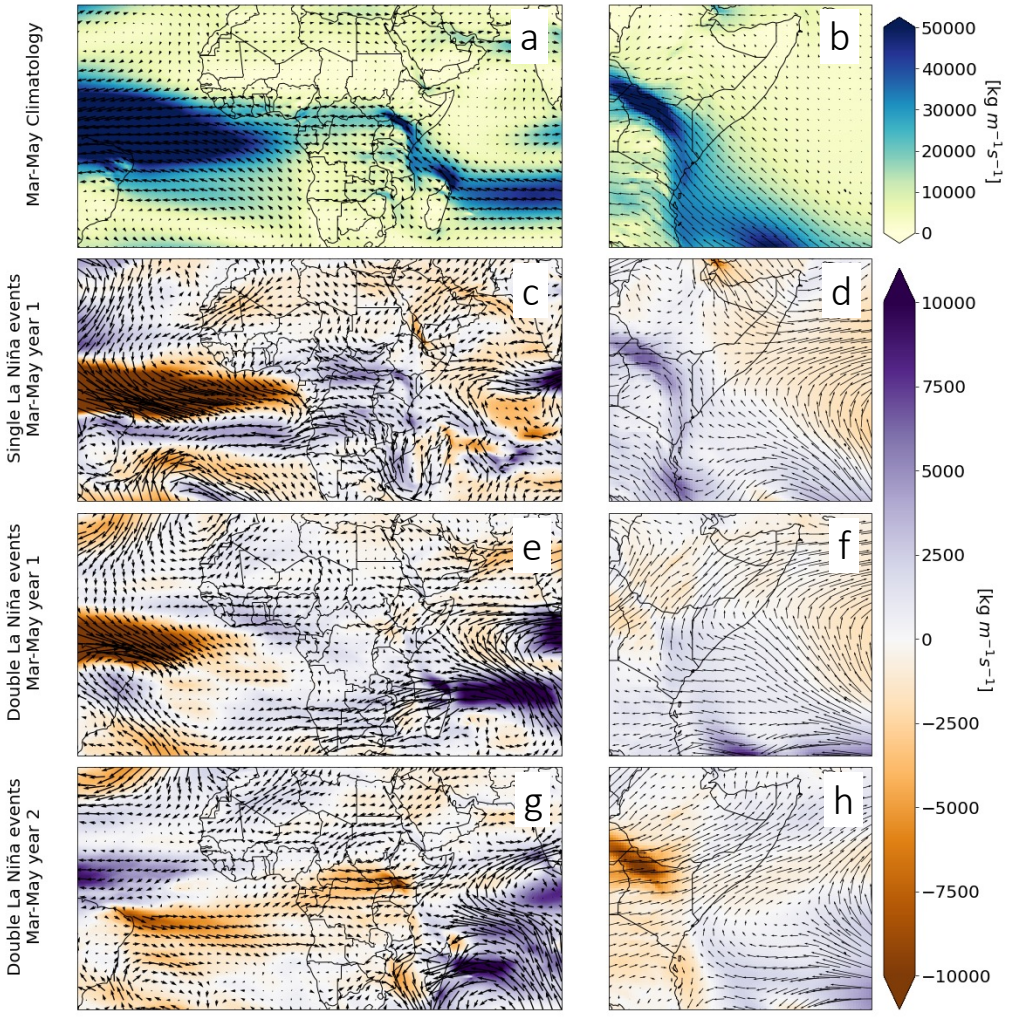

FIG. 7. Vertically integrated moisture transport - defined as moisture transport integrated from the surface of the Earth to the top of the atmosphere - climatology (a,b) and anomalies during single-year La Niñas (c,d), as well as during the first-year (e,f) and second-year (g,h) of multi-year La Niñas. Shading in each plot shows the magnitude of transport. In the c-h positive values indicate transport that enhances the mean-state transport while negative values indicate moisture transport that is in the opposite sense of the mean-state transport. The left column shows an all Africa domain, while the right column shows the same quantities over East Africa.

Accepted for publication in *Journal of Hydrometeorology*. DOI 10.1175/JHM-D-22-0043.1.

amount of moisture is moved westward through the Turkana channel and over Northern Tanzania out of the region, while during second-year events less moisture than normal is diverged out of the region across the continent, resulting in a greater net divergence of moisture out of the region during first-year events as compared to second-year events (Fig. 7c-h). To test how robust the relationship between Tropical South Atlantic SSTs and cross-continental moisture transport is, we created similar composites based on tropical South Atlantic SST anomalies during ENSO neutral Mar-May years, which showed that a warm tropical South Atlantic tends to be associated with greater east-to-west moisture transport as compared to years with a cool tropical South Atlantic (SI Fig. 6). These results agree with past analyses that observe greater cross-continental moisture transport and surface divergence over East Africa when the Tropical South Atlantic is warm and the Indian Ocean is cold (Camberlin and Okoola 2003; Okoola 1999a,b)

4. Discussion

We demonstrate that multi-year La Niña events favor drought in the Horn of Africa for three consecutive seasons (OND-MAM-OND), but that they do not tend to increase the probability of a fourth season of drought owing to the different sea surface temperatures and associated atmospheric teleconnections in the MAM long rains season following second-year La Niña events as compared to those following first-year La Niña events. During the long rains season following first-year La Niña events the ascending branches of the Walker Circulation are intensified over relatively warmer waters in the Tropical Atlantic and the West Pacific, while subsidence is increased over the Horn of Africa, which contributes to the observed dry conditions in those years. Second-year La Niña events, on the other hand, are associated with weaker ascent near 140E and enhanced atmospheric descent over the Indian Ocean rather than over the Horn of Africa and as a result the long rains are relatively wetter. The warmer tropical South Atlantic during first-year La Niñas as compared with second-year La Niñas is associated with increased cross-continental moisture transport out of East Africa and drier conditions in the Horn of Africa.

Atmospheric teleconnections during the long rains following first-year La Niñas are distinct from those following second-year La Niñas, therefore, due to differing sea surface temperatures throughout the tropics that affect the associated teleconnections. We note, however, that there exists substantial heterogeneity among second-year La Niña events in terms of both SST patterns and subsequent precipitation anomalies throughout the Horn of Africa. For example, second-year La Niñas have been associated with drought recently in 2000 and 2009 (Fig. S4). It is for this reason that we stress the importance of the SST patterns that are associated with drought conditions rather than the distinction between first-year and second-year La Niñas alone.

Accepted for publication in *Journal of Hydrometeorology*. DOI 10.1175/JHM-D-22-0043.1.

Our analysis is observationally-based, which has the benefit of circumventing persistent model deficiencies in simulating both the mean state and variability of rainfall in East Africa (Yang et al. 2014, 2015). Our observational approach, however, is limited by a relatively small sample size. We identified only 25 La Niña events over the entire observational record, of which sixteen were part of a double La Niña and nine were single La Niñas. Our conclusions, therefore, would benefit from being further evaluated in a modeling environment provided sufficient model skill in both the long rains and short rains seasons. In particular we highlight that a modeling environment could clarify the relative importance of a westward-shifted Walker Circulation as compared to an enhanced cross-continental moisture transport for drying East Africa during the long rains following first- and second-year La Niña events.

When considering these results, and future potential outcomes, it is important to note that the dramatic long-term drying of Mar-May rains in the Horn of Africa has been linked to ongoing warming in the West Pacific compared to the Central and East Pacific (Funk et al. 2019, 2018; Williams and Funk 2011; Lyon and DeWitt 2012; Funk and Hoell 2015). The observed strengthening of zonal SST gradients in the Pacific is consistent with a response to anthropogenic forcing known as the ocean dynamical thermostat mechanism (Clement et al. 1996; Seager et al. 2019). SST patterns favoring drought in the Horn of Africa may, therefore, continue to occur more frequently in the future compared to the first half of the twentieth century. Likewise, we may reasonably expect multi-season droughts to continue occurring at the relatively higher rates seen in the last twenty years (Hoell and Funk 2014), ensuring that they remain a major source of climate risk in East Africa. Past research has demonstrated that by using these zonal SST gradients in the Pacific droughts in Mar-May can be predicted as early as January Funk et al. (2014). Such forecasts were developed using a statistical approach based on SST indices Funk et al. (2014) and using climate analogs Shukla et al. (2014), both of which demonstrate greater skill in Mar-May than the coupled dynamical climate model-based forecasts of the time. Improving our understanding of and our ability to predict these droughts should be a priority for adapting to anthropogenic climate change.

Our results provide physical understanding of the sources and limitations of predictability stemming from multi-year La Niña forecasts in the Horn of Africa. Such forecasts would be of considerable value for predicting acute food insecurity given the climate sensitivity of livelihoods in the region. The majority of the areas that we identify as experiencing multi-year drought during mult-year La Niña events are pastoral or agropastoral livelihood zones. Agropastoralists in this region already use seasonal forecasts to inform planting and harvest decisions (Luseno et al. 2003), while nomadic pastoralist households often rely upon food aid during times of drought (Rufino et al. 2013). Multi-season forecasts would allow for the coordination of food aid policies that often

Accepted for publication in *Journal of Hydrometeorology*. DOI 10.1175/JHM-D-22-0043.1.

take months to complete, such as the direct shipment of grain to a region, as well as allowing agropastoral households to consider a wider variety of management strategies.

5. Data Availability Statement

All data used in this article are analyses of existing, publicly available datasets. GPCC and CRU precipitation data can be found at $https://psl.noaa.gov/data/gridded/data.gpcc.html$ and $https://crudata.uea.ac.uk/cru/data/hrg/$, respectively. ERA5 data is available from $https://cds.climate.copernicus.eu/$, HadISST data is from $https://www.metoffice.gov.uk/hadobs/hadisst/$, and GRUN runoff data from $https://doi.org/10.6084/m9.figshare.9228176$

6. Acknowledgements

We thank Andy Hoell and Laura Harrison for helpful conversations early in the development of this analysis. This publication was made possible through the support of the Bureau of Humanitarian Assistance, U.S. Agency for International Development, under the terms of PAPA AID-FFP-T-17-00001 FAMINE EARLYWARNING SYSTEMS NETWORK (FEWS NET).

References

Anderson, W., and Coauthors, 2021: Violent conflict exacerbated drought-related food insecurity between 2009 and 2019 in sub-saharan africa. *Nature Food*, **2 (8)**, 603–615.

Barnston, A. G., M. K. Tippett, M. L. L'Heureux, S. Li, and D. G. DeWitt, 2012: Skill of real-time seasonal enso model predictions during 2002–11: Is our capability increasing? *Bulletin of the American Meteorological Society*, **93 (5)**, 631–651.

Barnston, A. G., M. K. Tippett, M. Ranganathan, and M. L. L'Heureux, 2019: Deterministic skill of enso predictions from the north american multimodel ensemble. *Climate Dynamics*, **53 (12)**, 7215–7234.

Behera, S. K., J.-J. Luo, S. Masson, P. Delecluse, S. Gualdi, A. Navarra, and T. Yamagata, 2005: Paramount impact of the indian ocean dipole on the east african short rains: A cgcm study. *Journal of Climate*, **18 (21)**, 4514–4530.

Blau, M., and K.-J. Ha, 2020: The indian ocean dipole and its impact on east african short rains in two cmip5 historical scenarios with and without anthropogenic influence. *Journal of Geophysical Research: Atmospheres*, **125 (16)**, e2020JD033 121.

Camberlin, P., and R. Okoola, 2003: The onset and cessation of the "long rains" in eastern africa and their interannual variability. *Theoretical and Applied Climatology*, **75 (1)**, 43–54.

Clement, A. C., R. Seager, M. A. Cane, and S. E. Zebiak, 1996: An ocean dynamical thermostat. *Journal of Climate*, **9 (9)**, 2190–2196.

DiNezio, P. N., and C. Deser, 2014: Nonlinear controls on the persistence of la niña. *Journal of Climate*, **27 (19)**, 7335–7355.

DiNezio, P. N., C. Deser, Y. Okumura, and A. Karspeck, 2017a: Predictability of 2-year la niña events in a coupled general circulation model. *Climate dynamics*, **49 (11)**, 4237–4261.

DiNezio, P. N., and Coauthors, 2017b: A 2 year forecast for a 60–80% chance of la niña in 2017–2018. *Geophysical Research Letters*, **44 (22)**, 11–624.

Dutra, E., L. Magnusson, F. Wetterhall, H. L. Cloke, G. Balsamo, S. Boussetta, and F. Pappenberger, 2013: The 2010–2011 drought in the horn of africa in ecmwf reanalysis and seasonal forecast products. *International Journal of Climatology*, **33 (7)**, 1720–1729.

FEWSNET, 2021: The eastern horn of africa faces an exceptional prolonged and persistent agro-pastoral drought sequence. Tech. rep., The IGAD Climate Prediction and Applications Center (ICPAC), the Famine Early Warning Systems Network (FEWS NET), the Food and Agriculture Organization Global Information and Early Warning System (FAO GIEWS), the World Food Programme (WFP) and the Joint Research Center (JRC).

Funk, C., A. Hoell, S. Shukla, I. Blade, B. Liebmann, J. B. Roberts, F. R. Robertson, and G. Husak, 2014: Predicting east african spring droughts using pacific and indian ocean sea surface temperature indices. *Hydrology and Earth System Sciences*, **18 (12)**, 4965–4978.

Funk, C., and Coauthors, 2018: Examining the role of unusually warm indo-pacific sea-surface temperatures in recent african droughts. *Quarterly Journal of the Royal Meteorological Society*, **144**, 360–383.

Funk, C., and Coauthors, 2019: Examining the potential contributions of extreme "western v" sea surface temperatures to the 2017 march–june east african drought. *Bulletin of the American Meteorological Society*, **100 (1)**, S55–S60.

Funk, C. C., and A. Hoell, 2015: The leading mode of observed and cmip5 enso-residual sea surface temperatures and associated changes in indo-pacific climate. *Journal of Climate*, **28 (11)**, 4309–4329.

Accepted for publication in *Journal of Hydrometeorology*. DOI 10.1175/JHM-D-22-0043.1.

Ghiggi, G., V. Humphrey, S. I. Seneviratne, and L. Gudmundsson, 2019: Grun: an observation-based global gridded runoff dataset from 1902 to 2014. *Earth System Science Data*, **11 (4)**, 1655–1674.

Gleixner, S., T. Demissie, and G. T. Diro, 2020: Did era5 improve temperature and precipitation reanalysis over east africa? *Atmosphere*, **11 (9)**, 996.

Goddard, L., and N. E. Graham, 1999: Importance of the indian ocean for simulating rainfall anomalies over eastern and southern africa. *Journal of Geophysical Research: Atmospheres*, **104 (D16)**, 19 099–19 116.

Ham, Y.-G., J.-H. Kim, and J.-J. Luo, 2019: Deep learning for multi-year enso forecasts. *Nature*, **573 (7775)**, 568–572.

Harris, I., T. J. Osborn, P. Jones, and D. Lister, 2020: Version 4 of the cru ts monthly high-resolution gridded multivariate climate dataset. *Scientific data*, **7 (1)**, 1–18.

Hastenrath, S., D. Polzin, and C. Mutai, 2011: Circulation mechanisms of kenya rainfall anomalies. *Journal of Climate*, **24 (2)**, 404–412.

Hersbach, H., and Coauthors, 2020: The era5 global reanalysis. *Quarterly Journal of the Royal Meteorological Society*, **146 (730)**, 1999–2049.

Hoell, A., and C. Funk, 2013: The enso-related west pacific sea surface temperature gradient. *Journal of Climate*, **26 (23)**, 9545–9562.

Hoell, A., and C. Funk, 2014: Indo-pacific sea surface temperature influences on failed consecutive rainy seasons over eastern africa. *Climate dynamics*, **43 (5-6)**, 1645–1660.

Hoell, A., C. Funk, and M. Barlow, 2014: The regional forcing of northern hemisphere drought during recent warm tropical west pacific ocean la niña events. *Climate dynamics*, **42 (11-12)**, 3289–3311.

Jong, B.-T., M. Ting, R. Seager, and W. B. Anderson, 2020: Enso teleconnections and impacts on us summertime temperature during a multiyear la niña life cycle. *Journal of Climate*, **33 (14)**, 6009–6024.

Lenssen, N. J., L. Goddard, and S. Mason, 2020: Seasonal forecast skill of enso teleconnection maps. *Weather and Forecasting*, **35 (6)**, 2387–2406.

Liebmann, B., and Coauthors, 2014: Understanding recent eastern horn of africa rainfall variability and change. *Journal of Climate*, **27 (23)**, 8630–8645.

Accepted for publication in *Journal of Hydrometeorology*. DOI 10.1175/JHM-D-22-0043.1.

Liebmann, B., and Coauthors, 2017: Climatology and interannual variability of boreal spring wet season precipitation in the eastern horn of africa and implications for its recent decline. *Journal of Climate*, **30 (10)**, 3867–3886.

Liu, W., K. H. Cook, and E. K. Vizy, 2020: Influence of indian ocean sst regionality on the east african short rains. *Climate Dynamics*, **54 (11)**, 4991–5011.

Luo, J.-J., G. Liu, H. Hendon, O. Alves, and T. Yamagata, 2017: Inter-basin sources for two-year predictability of the multi-year la niña event in 2010–2012. *Scientific reports*, **7 (1)**, 1–7.

Luseno, W. K., J. G. McPeak, C. B. Barrett, P. D. Little, and G. Gebru, 2003: Assessing the value of climate forecast information for pastoralists: Evidence from southern ethiopia and northern kenya. *World development*, **31 (9)**, 1477–1494.

Lyon, B., and D. G. DeWitt, 2012: A recent and abrupt decline in the east african long rains. *Geophysical Research Letters*, **39 (2)**.

Maxwell, D., and P. Hailey, 2020: The politics of information and analysis in famines and extreme emergencies synthesis of findings from six case studies. Tech. rep., Feinstein International Center.

Maxwell, D. G., and N. Majid, 2016: *Famine in Somalia: Competing imperatives, collective failures, 2011-2012*. Oxford University Press.

Nicholson, S. E., 2017: Climate and climatic variability of rainfall over eastern africa. *Reviews of Geophysics*, **55 (3)**, 590–635.

Okoola, R. E., 1999a: A diagnostic study of the eastern africa monsoon circulation during the northern hemisphere spring season. *International Journal of Climatology: A Journal of the Royal Meteorological Society*, **19 (2)**, 143–168.

Okoola, R. E., 1999b: Midtropospheric circulation patterns associated with extreme dry and wet episodes over equatorial eastern africa during the northern hemisphere spring. *Journal of Applied Meteorology and Climatology*, **38 (8)**, 1161–1169.

Okumura, Y. M., and C. Deser, 2010: Asymmetry in the duration of el niño and la niña. *Journal of Climate*, **23 (21)**, 5826–5843.

Okumura, Y. M., P. DiNezio, and C. Deser, 2017: Evolving impacts of multiyear la niña events on atmospheric circulation and us drought. *Geophysical Research Letters*, **44 (22)**, 11–614.

Accepted for publication in *Journal of Hydrometeorology*. DOI 10.1175/JHM-D-22-0043.1.

Rao, M. P., E. R. Cook, B. I. Cook, K. J. Anchukaitis, R. D. D'Arrigo, P. J. Krusic, and A. N. LeGrande, 2019: A double bootstrap approach to superposed epoch analysis to evaluate response uncertainty. *Dendrochronologia*, **55**, 119–124.

Rasmusson, E. M., and T. H. Carpenter, 1982: Variations in tropical sea surface temperature and surface wind fields associated with the southern oscillation/el niño. *Monthly Weather Review*, **110 (5)**, 354–384.

Rayner, N., D. E. Parker, E. Horton, C. K. Folland, L. V. Alexander, D. Rowell, E. C. Kent, and A. Kaplan, 2003: Global analyses of sea surface temperature, sea ice, and night marine air temperature since the late nineteenth century. *Journal of Geophysical Research: Atmospheres*, **108 (D14)**.

Rufino, M. C., P. K. Thornton, I. Mutie, P. Jones, M. Van Wijk, M. Herrero, and Coauthors, 2013: Transitions in agro-pastoralist systems of east africa: impacts on food security and poverty. *Agriculture, ecosystems & environment*, **179**, 215–230.

Saji, N., and T. Yamagata, 2003: Possible impacts of indian ocean dipole mode events on global climate. *Climate Research*, **25 (2)**, 151–169.

Schneider, U., A. Becker, P. Finger, A. Meyer-Christoffer, and M. Ziese, 2018: Gpcc full data monthly product version 2018 at 0.5°: Monthly land-surface precipitation from rain-gauges built on gts-based and historical data. *Global Precipitation Climatology Centre*.

Seager, R., M. Cane, N. Henderson, D.-E. Lee, R. Abernathey, and H. Zhang, 2019: Strengthening tropical pacific zonal sea surface temperature gradient consistent with rising greenhouse gases. *Nature Climate Change*, **9 (7)**, 517–522.

Shukla, S., C. Funk, and A. Hoell, 2014: Using constructed analogs to improve the skill of national multi-model ensemble march–april–may precipitation forecasts in equatorial east africa. *Environmental Research Letters*, **9 (9)**, 094 009.

Shukla, S., G. Husak, W. Turner, F. Davenport, C. Funk, L. Harrison, and N. Krell, 2021: A slow rainy season onset is a reliable harbinger of drought in most food insecure regions in sub-saharan africa. *Plos one*, **16 (1)**, e0242 883.

Shukla, S., J. Roberts, A. Hoell, C. C. Funk, F. Robertson, and B. Kirtman, 2019: Assessing north american multimodel ensemble (nmme) seasonal forecast skill to assist in the early warning of anomalous hydrometeorological events over east africa. *Climate Dynamics*, **53 (12)**, 7411–7427.

Tierney, J. E., J. E. Smerdon, K. J. Anchukaitis, and R. Seager, 2013: Multidecadal variability in east african hydroclimate controlled by the indian ocean. *Nature*, **493 (7432)**, 389–392.

Tokinaga, H., I. Richter, and Y. Kosaka, 2019: Enso influence on the atlantic niño, revisited: Multi-year versus single-year enso events. *Journal of Climate*, **32 (14)**, 4585–4600.

Ummenhofer, C. C., M. Kulüke, and J. E. Tierney, 2018: Extremes in east african hydroclimate and links to indo-pacific variability on interannual to decadal timescales. *Climate dynamics*, **50 (7)**, 2971–2991.

Williams, A. P., and C. Funk, 2011: A westward extension of the warm pool leads to a westward extension of the walker circulation, drying eastern africa. *Climate Dynamics*, **37 (11)**, 2417–2435.

Wu, X., Y. M. Okumura, C. Deser, and P. N. DiNezio, 2021: Two-year dynamical predictions of enso event duration during 1954–2015. *Journal of Climate*, **34 (10)**, 4069–4087.

Wu, X., Y. M. Okumura, and P. N. DiNezio, 2019: What controls the duration of el niño and la niña events? *Journal of Climate*, **32 (18)**, 5941–5965.

Yang, W., R. Seager, M. A. Cane, and B. Lyon, 2014: The east african long rains in observations and models. *Journal of Climate*, **27 (19)**, 7185–7202.

Yang, W., R. Seager, M. A. Cane, and B. Lyon, 2015: The annual cycle of east african precipitation. *Journal of Climate*, **28 (6)**, 2385–2404.

Zebiak, S. E., and M. A. Cane, 1987: A model el niñ–southern oscillation. *Monthly Weather Review*, **115 (10)**, 2262–2278.